

A NOVEL HYBRID FC-BATTERY DRIVE SYSTEM FOR ELECTRIC VEHICLES

E. Elbakush, Student Member IEEE

Dept. of Electrical and Computer Engineering
University of New Brunswick, Canada
E-mail: e.elbakush@unb.ca

A. M. Sharaf, Senior Member IEEE

Energy Research Group
University of Trinidad and Tobago UTT
E-mail: adel.sharaf@utt.edu.tt

ABSTRACT

The paper presents the dynamic modeling and coordinated control strategy for an integrated Electric Vehicle drive scheme using Fuel Cell (FC) and Battery back up. The integrated DC drive Scheme is fully stabilized using a novel FACTS based green filter compensator that ensures a fully stabilized Common-DC Bus voltage with reduced inrush current conditions under source and load excursions. The Fuel Cell and Battery are utilized efficiently using the error driven multi loop control strategy. The dynamic Filter Compensator Scheme is validated using the Modified Tri-loop PID controller developed by the Second Author to control the DC-DC converter and Green Power Filter Compensator (GPFC). The paper presents the validation of the multi loop Modified PID controller for the Hybrid FC and Battery E V powered four-wheel DC drive using Permanent Magnet DC (PMDC) motors. The model includes DC drive and load nonlinearities in inertia (J) and viscous friction (B). A Tri-Loop dynamic error controller is used to regulate the motor inrush current and overloading conditions, in addition to speed dynamic reference tracking. A type (B) DC-DC converter is employed to control the power transfer from the Fuel Cell and Battery to the PMDC motor load. All Matlab-Simulink Digital Simulation Functional Models for the Fuel Cell, battery, DC-DC converter, PMDC motor, interface LC-Filters, and Controller Loops are fully modeled using MATLAB/SIMULINK/Sim-power Software Environment.

Index Terms— Fuel Cell, PMDC Drives, GPFC Filter Compensator, Electric Vehicles, Tri-loop Error Driven Controller.

1. INTRODUCTION

The increasing demand for efficient energy utilization, green power use renewable and green energy sources (Wind, Solar, PV, Wave, Tidal, Fuel Cell, Biogas, Hybrid..) is motivated by economic and environmental concerns. The increasing reliance on fossil fuels with increasing rate of Hydro Carbon resource depletion is causing a strategic shift to energy alternatives, clean fuel replacement and energy displacement of conventional sources to new green renewable, environmentally safe and friendly counterparts [1]-[2].

Photovoltaic and wind generation schemes are considered to be the most viable and economic choices for micro grid electrical energy generation [3]. The growing demand for the electrical energy throughout the world has motivated the use of new renewable sources of energy. Among the unconventional renewable energy sources that have been studied, Fuel Cell energy is now becoming a promising viable and economical renewable/alternative energy source. Except for its higher initial installation costs, the PV energy has many advantages: it is reliable and requires little maintenance. It costs little to operate and almost has no environmental impact. It's both modular and flexible in terms of economical sizes and ranges of appli-

cations Battery powered electric vehicles (BEVs) have zero vehicle emissions at the place of use. Lifecycle emissions depend on the electricity generation technology but reductions in both local and global pollutants can be achieved. Maintenance requirements are low and the reliability is high. Fuel costs are low. BEVs are quiet and have low vibrations. Electric vehicles can draw their energy from a variety of primary sources [1]. Various studies on electric vehicle Fuel Cell systems can be found in literature [2]-[3].

Fuel Cells are devices that convert the chemical energy of hydrogen, methanol or other chemical compounds directly into electricity, without any combustion or thermal cycles. The process is that of electrolysis in reverse. Because hydrogen and oxygen gases are electrochemically converted into water, Fuel Cells have many advantages over heat engines. These include: high efficiency, virtually silent operation and, if hydrogen is the fuel, there are no pollutant gaseous emissions. If the hydrogen is also produced from renewable photovoltaic or wind energy sources, then the electrical power produced can be truly sustainable.

Currently Fuel Cell Battery research is concentrating on the development of efficient and safe low-temperature Fuel Cell technology. Enhancing the Fuel Cell output efficiency and improving the unified system performance are among main research topics [3]. DC motor is one of the machines convert the electrical energy to the mechanical energy. Nowadays, DC motor drive systems are widely used in many industries [1]. Years ago, most of the servomotors used for position control runs with alternative current (AC). DC motors are preferred in some applications due to difficulties of control and nonlinearity of AC motors. However, because of the brush and commutator inside DC motor, the maintenance is more difficult and more expensive. Thanks to development of permeant Magnet DC motor technology and power electronics, moment per volume of the motor has increased and permanent magnet motor types have been advanced. Thus the brush and commutator maintenance drawbacks have been eliminated.

The DC motor speed or position control can be realized using control methods that include conventional PI, PID, fuzzy logic based, nonlinear, adaptive variable structure, model reference adaptive control, artificial neural networks, feed-forward computed torque control strategies [8].

2. SYSTEM DESCRIPTION

The proposed four-wheel PMDC electric vehicle drive system is shown in Fig.1. The proposed system consists of four parts. There are DC voltage supply like a Fuel Cell (FC) and a Battery, DC-DC Chopper, a controller and four PMDC motors for wheels. In this study, Fuel Cell and Battery constant DC voltage supply giving the required voltage and current ratings, type B chopper and PMDC mo-

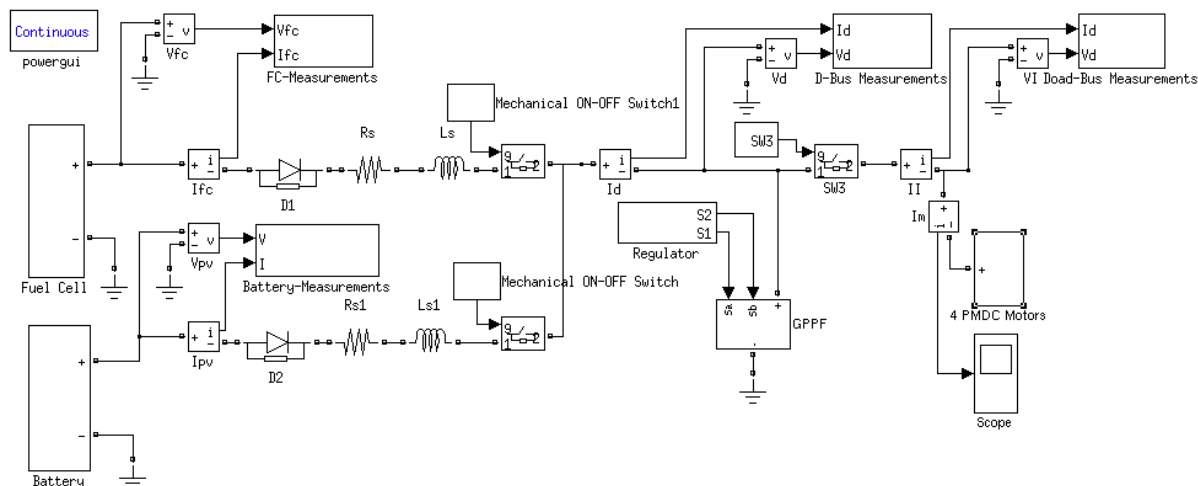


Fig. 1. Hybrid Fuel Cell FC-Battery drive scheme for Electric Vehicle DC Drive.

tor are used. The Fuel Cell and the Battery are used all the time. The schematic diagram of prototype four-wheel drive electric vehicle is shown in Fig.1. The proposed cottage FC and Battery energy system has the following parts:

1. The Electrochemical voltage behaviour of the Fuel Cell is com-

4. Input side Capacitor (C1): It's a large value capacitor works as storage media.
5. Loads: Here the loads are four dc motors such as the Permanent Magnet DC motor used in the simulation [3]-[4].
6. Green Plug Power Filter.

3. GREEN PLUG POWER FILTER GPFC

In order to enhance the unified Hybrid Fuel Cell and Battery motor derive system performance a green plug capacitor filter GPFC comprising switchable capacitor is introduced at the DC bus. The GPPF is also controlled to absorb ripple and reduce DC side current oscillations. The idea behind the controller is to detect major excursions in the motor measurements and feed the errors to a PWM module that in turn generates the switching pulses to the filter switches in accordance with the duty ratio and the error value [5]. The GPPF used and tested with the operation of the electric motor is shown in Fig.3.

The GPFC control scheme developed by the Second Author is based on a decoupled current and voltage components of the DC bus. The GPFC must be connected across the DC bus terminal to maintain constant DC voltage in order to allow operation of the VSC-converter with three control loops as shown as Simulink model in Fig.6. The primary duty of the capacitor bank is to provide a voltage path, current path as well as power path as shown in Fig.6. The input of control loop 1 is the bus voltage, which produces an error with respect to the measured value and then, the error is used for voltage regulation. The input to loop 2 is the bus current that has the same transfer function as the voltage loop. The input to loop 3 is the power loop that has the same transfer function as the voltage loop. The increased capacity of power electronic converters used in GPFC also allows for adequate sizing and optimized operation [7]-[8]. In this paper the effectiveness of the GPFC scheme is fully validated using Matlab/Simulink digital simulation. All of the subsystem components used in the effective Hybrid FC and Battery powered four PMDC motors used in electric vehicle are sub-modeled individually using the Matlab/Simulink GUI environment and combined to establish the overall system model. The simulation of the proposed scheme has been carried out and the dynamic performance of the system is examined for the control validation.

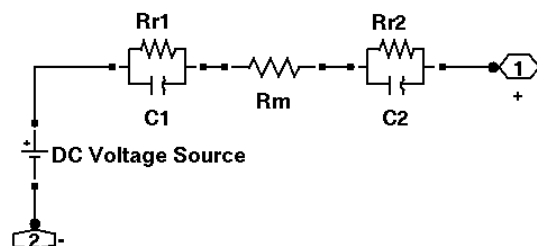


Fig. 2. Electrical equivalent DC circuit of Fuel Cell.

monly modeled using the simple equivalent first order circuit shown in Fig.2. This circuit consist three passive circuit elements that result in a first order approximation of the dynamic response of the electrochemical capacitor. The circuit includes the double layer capacitance C_1 , R_{r1} , R_m , C_2 , R_{r2} . The equivalent series resistance that represents the energy lost due to the distributive resistance of the electrolyte, electronic contacts and the porous separator [3]. R_m is the ohmic resistance in the electrolyte. R_1 is the charge transfer resistance between the electrolyte and anode while C_1 is the charge due to the double layer present at the anode surface. Similarly, R_1 is the charge transfer resistance between the electrolyte and cathode while C_2 is the charge due to the double layer present at the cathode surface.

2. Battery.
3. Power isolation and source filtering.
 - a) Blocking Diode: To block the reverse current flow.
 - b) DC side filter (R_f , L_f): The DC side filter allows for a valid quasi static model of the Fuel Cell and ensures sufficient time scale decoupling of the three supplementary control loop.
 - c) Type B MOSFET or IGBT DC-DC converter (Chopper) using Pulse Width Modulated (PWM) switching circuit.

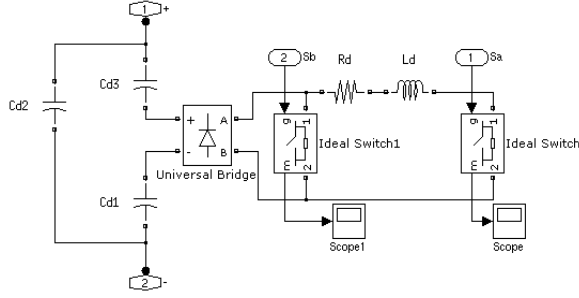


Fig. 3. Green Plug Power Filter (GPPF) for stabilizing Common DC Bus voltage.

4. DC MOTOR

Permanent Magnet DC motors have desirable properties and features. Some of them are reliability, durable, Low cost, and low operation voltages, having positive conversion coefficients between electrical and mechanical components, having size and design variation. A permanent magnet dc motor (PMDC) is one of the DC motor types. PMDC system converts electrical power provided by a voltage source to mechanical power provided by a spinning rotor by means of magnetic coupling. The equivalent circuit of a PMDC motor is illustrated in Fig.4. The parameters and symbols, which were used in simulating the system, are given in Appendix. The armature coil

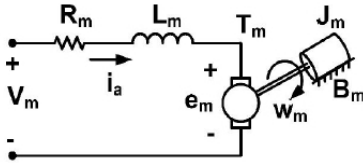


Fig. 4. The equivalent circuit of the PMDC motor.

of the DC motor can be represented by an inductance (L_m) in series with resistance (R_m) and with a series induced voltage (e_m), which opposes the voltage source. Using Kirchhoffs voltage law around the electrical loop can derive a differential equation for the equivalent circuit.

$$V_m(k) = R_m i_a(k) + L_m \frac{dI_a}{dt} + e_m(k) \quad (1)$$

where:

$$e_m(k) = K_E \cdot \omega_m(k), i_a = \text{Constant}; \text{ there for } K_E = K_T$$

The sum of the torques of the motor must be equal zero, therefor,

$$T_e(t) - J \frac{d\omega_m(k)}{dt} - B\omega_m(k) - T_L(t) = 0 \quad (2)$$

The electromagnetic torque is proportional to the current though the armature winding and can be written as

$$T_e(k) = K_T \cdot i_a \quad (3)$$

The load torque is given by the nonlinear equation (9)

$$T_L = K_0 + K_1 \omega_m + K_2 \omega_m^2 \quad (4)$$

Where, the coefficients K_0 , K_1 and K_2 are chosen as given in the Appendix. The differential equations in state space form for the armature current and angular velocity can be written as

$$\frac{d}{dt} \begin{bmatrix} i_a \\ \omega_m \end{bmatrix} = \begin{bmatrix} -\frac{R_m}{L_m} & -\frac{K_T}{L_m} \\ \frac{K_T}{J} & -\frac{B}{J} \end{bmatrix} \begin{bmatrix} i_a \\ \omega_m \end{bmatrix} + \begin{bmatrix} \frac{1}{L_m} & 0 \\ 0 & -\frac{1}{J} \end{bmatrix} \begin{bmatrix} V_m \\ T_L \end{bmatrix} \quad (5)$$

Where i_a and ω_m are motor armature current and speed.

The values of the parameters used in PMDC motor modelling are given in the Appendix. Load torque is taken as generalized nonlinear Torque term.

$$T_L(\omega_m) = 1.48 + 7.4e^{-3}\omega_m + 8.14e^{-5}\omega_m^2 \quad (6)$$

The nonlinear inertia J and B viscous friction have the following forms and the values of those parameters are given in the Appendix:

$$\begin{aligned} J(\omega_m) &= J_0 + J_1 |\omega_{mpu}|^2 \\ B(\omega_m) &= B_0 + B_1 |\omega_{mpu}|^2 \end{aligned} \quad (7)$$

Where, the coefficients B_0, B_1, B_2, J_0, J_1 and J_2 are chosen as given in appendix[4].

5. DYNAMIC ERROR DRIVEN CONTROL

In this paper, the novel Modified Tri-loop error driven dynamic controller scheme shown in Fig.5 is implemented for speed control of the PMDC motor, which comprises three basic loops, namely the main speed stabilization loop, the motor current dynamic error loop, and the supplementary dynamic momentum-tracking loop. The additional dynamic loops ensure energy efficient utilization and reduced current ripple content. The novel Modified Tri-loop error driven dynamic controller scheme shown in Fig.5 is implemented for GPPF controlled to control absorb ripple and reduce DC side current oscillations, which comprises three basic loops, namely the main voltage stabilization loop, current dynamic error loop, and the power loop.

1. The speed variation from its reference values is the main loop for voltage stabilization. The control signal weight γ_S is selected as 3.5.

2. The load current is the dynamic error coordinative type minimum load current excursion from maximum motor current. The weight γ_I is selected as 1.3, to include the changes and excursions in load current.

3. The dynamic momentum loop with the weight γ_R selected as 0.83 to minimum excursion of motor momentum.

The total error signal (e_t) is the sum of these three basic dynamically scaled loop errors that presents by:

$$e_t = \gamma_S \cdot e_S + \gamma_I \cdot e_I + \gamma_R \cdot e_R \quad (8)$$

The system control signal has the following form in the time domain:

$$V_c(t) = \gamma_1 e_t(t) + \gamma_2 \int_0^t e_t(t) dt + \gamma_3 \int_0^t (e_t(t))^2 dt \quad (9)$$

The tri-loop architecture compensate for any dynamic oscillations in Common DC bus voltage, motor current at the DC bus. The loop weighing factors are assigned to ensure loop time scaling and dominant loop control action. The total error signal to ensure maximum power utilization of the Tri-loop is driven through a PID controller

that is used to compensate the dynamic total error in order to provide the control signal required for GPFC switching. This control signal is used to adjust the Pulse Width Modulated (PWM) generator through saturation to adjust the sequence of the IGBT/Diode switch triggering which is shown in Fig.6. The control PID gains (K_p , K_i , and K_d) are selected to minimize an objective function, voltage stabilization and efficient energy utilization [6]. The novel tri-loop dynamic decoupled controller is validated for voltage stabilization and dynamic reactive compensation using MATLAB/SIMULINK/Sim-power Software Environment.

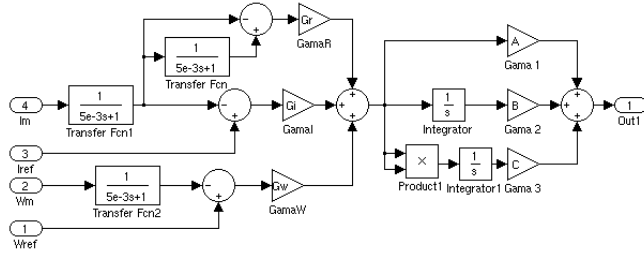


Fig. 5. Multi loop modified PID speed regulator for the DC-DC type (B) converter.

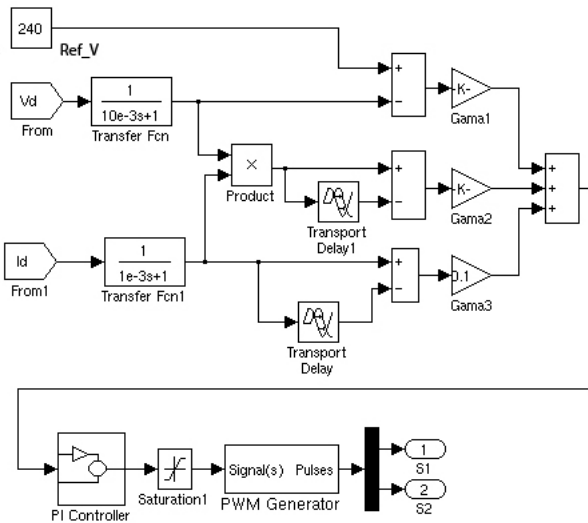


Fig. 6. Modified PID tri-loop dynamic controller with error squared compensation loop.

6. DIGITAL SIMULATION RESULTS

Hybrid DC Fuel Cell (FC) and Battery sources feeding the EV DC Drive scheme is subjected to four PMDC motors torque disturbances. The dynamic motor torque is increased by increasing the speed at $t = 4s$ and decreased by decreasing the speed at $t = 7s$. The Hybrid Fuel Cell (FC) and Battery unified controlled drive system is using the tri-loop error driven dynamic controller.

Fig.7 shows the digital simulation of the unified system dynamic responses of DC-bus voltage, Figures (8, 9, 10, 11, 12 and 13) show

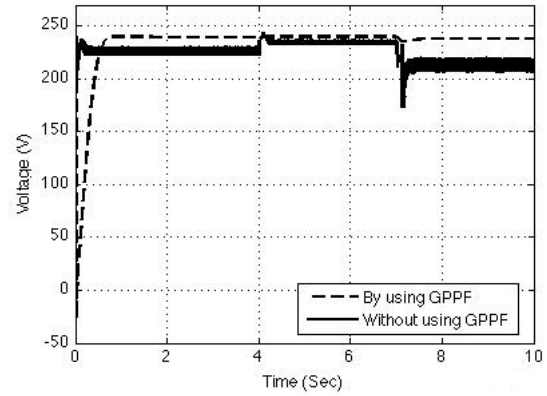


Fig. 7. Common DC Bus voltage dynamic response using the tri-loop GPFC PID controller.

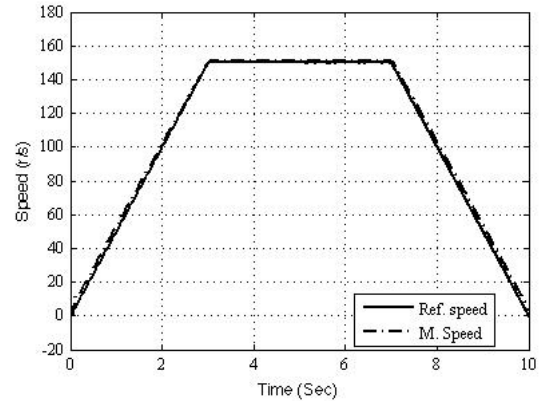


Fig. 8. Dynamic Speed reference response of PMDC motor using proposed modified tri-loop controller for type (B) DC-DC Converter.

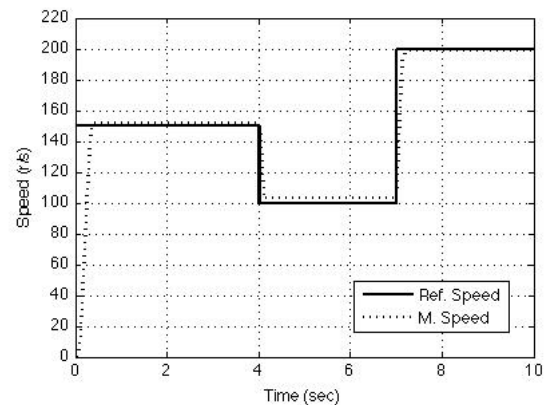


Fig. 9. Dynamic Speed reference response of PMDC motor using the modified tri-loop controller.

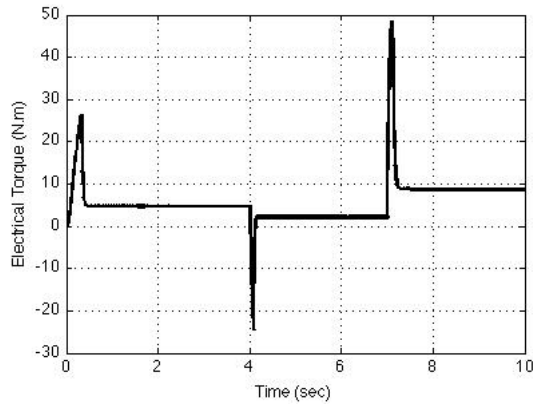


Fig. 10. Dynamic torque response of PMDC motors using the modified tri-loop PID controller.

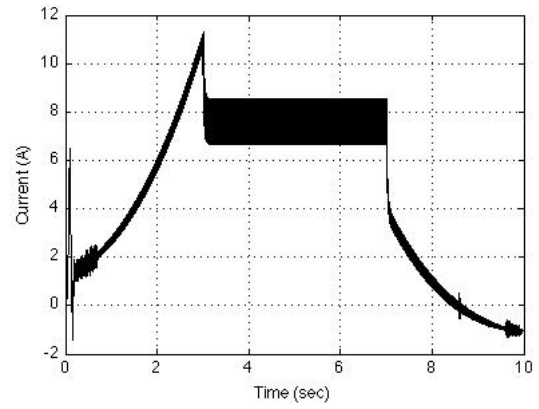


Fig. 13. PMDC motor current using the modified tri-loop PID controller.

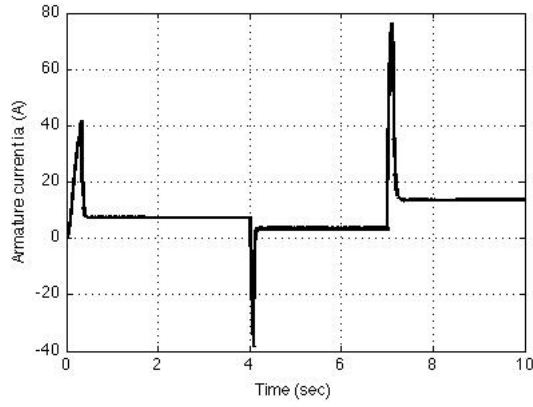


Fig. 11. PMDC motor current using the modified tri-loop PID controller.

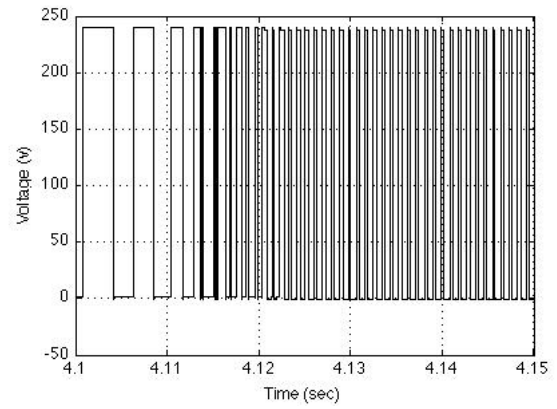


Fig. 14. PMDC motor modulated stator armature voltage.

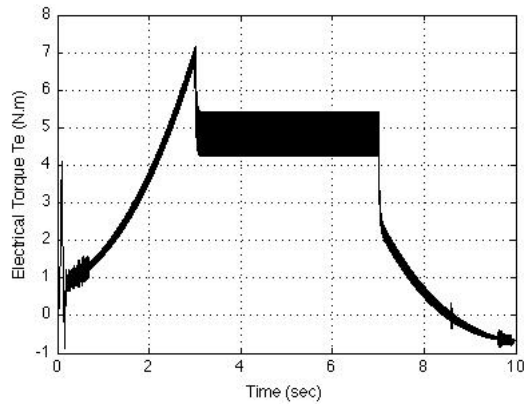


Fig. 12. Dynamic motor torque response using the modified tri-loop PID controller.

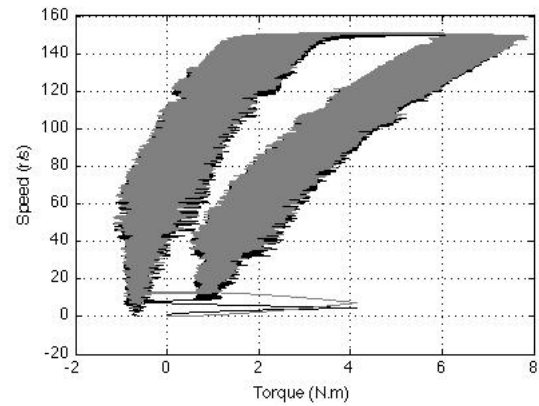


Fig. 15. Speed-vs-Torque dynamic response.

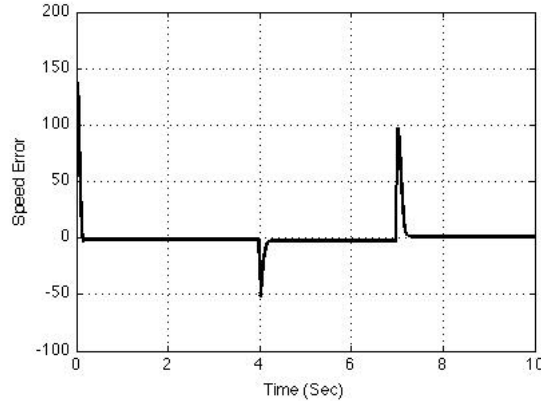


Fig. 16. Total controller error dynamic response.

PMDC motor speed, current, and torque using the proposed Modified controller. Figures (14 and 15) show the output signal to the DC-DC converter using the modified controller and the relation between the torque and the speed. The results indicated that the modified controller is effective in damping current and voltage excursions. The controller effectiveness in tracking different speed reference trajectories were tested for step and ramp reference. The error excursions are depicted. The PMDC motor starting speed, for a unit step change in the reference speed equals 150 r/s to 100 r/s and up to 200 r/s. The values of the gains γ_1 , γ_2 and γ_3 corresponding to the best solution obtained are used in the block diagram shown in Fig.5. Even though the design of the gains γ_1 , γ_2 and γ_3 are carried out assuming that there is no change in reference speed, the values of the gains γ_1 , γ_2 and γ_3 are used to study the system's response when there is a step change in reference speed. The response of speed track.

7. CONCLUSION

A novel DC hybrid Fuel Cell-Battery (EV-DC) Drive Scheme with equipped the novel coordinated control strategy developed by the Second Author is validated using MATLAB/SIMULINK Software Environment. The integrated Common DC - Bus scheme is fed by DC Fuel Cell FC and Battery and fully stabilized using a FACTS based Green Plug Filter Compensator (GPFC) to ensure a stabilized Common DC bus voltage with damped inrush current conditions under DC Source and Load excursions. The Fuel Cell and Battery excursions are compensated for by using the Green Plug Filter Compensator and the coordinated dynamic controller to ensure efficient EV-DC drive operation. The paper also presents a new version of a Modified PID controller to control the DC-DC converter Pulse Width Modulation and the Green Plug Filter Compensator (GPFC) using dynamic error driven Modified PID controller for the Hybrid FC and Battery powered four-wheel EV-DC drive. Motor models include mechanical and torque nonlinearities in combined inertia (J) and viscous friction (B). A Tri-Loop dynamic error driven speed regulation scheme is used to track reference speed with minimal inrush currents and overloading conditions. A type (B) two quadrant DC-DC converter is employed to control the power transfer from the Fuel Cell and the Battery to the PMDC motor load. The unified DC drive system is validated using the MATLAB/SIMULINK/Sim-power Software Environment under DC load excursions and motor torque changes. Hybrid Fuel Cell (FC) and Battery EV-DC drive with Green Plug Filter Compensator (GPFC) and coordinated multi

regulator error driven multi loop controllers were validated for efficient DC source utilization of Fuel Cell and Battery sources and dynamic speed reference tracking with minimal inrush currents and overloading conditions. The same GPFC scheme can be utilized with PV-Solar powered renewable green energy systems and DC-AC Renewable Energy utilization Schemes.

8. REFERENCES

- [1] B. Delfino, F. Fornari "Modeling and control of an integrated fuel-cell wind turbine system", *IEEE Power Tech. Conference Proceeding, Bologna* vol.2, pp. 23-26, June 2002
- [2] J. Correa, F. Farret, L. Canha, and M. Simoes, "An electrochemical-based fuel cell model suitable for electrical engineering automation approach". *IEEE Transaction on Industrial Electronics* vol. 51, issue 5, pp 1103-1112 Oct. 2004.
- [3] Sharaf, A.M, El-Sayed Mohamed A.H. "Dynamic Control of Fuel Cell Powered Water Pumping Station.", *International Conference on Renewable Energies and Power Quality (ICREPQ09)*, 2009
- [4] Elbakush, E., Sharaf, A. M and Altas I. "An Efficient Tri-Loop Controller for Photovoltaic Powered Four-Wheel Electric Vehicle.", *Innovations in Information Technology*, 200. IIT07., 2008, pp. 421-425.
- [5] A. M. Sharaf, R. Chhetri, "A novel dynamic capacitor compensator/green plug scheme for 3-phase 4-wire utilization loads", *IEEE-CCECE*, Ottawa, Ontario, Canada, 2006, pp. 454-459.
- [6] H. Fargali, F. Fahmy, and M. A. El-Sayed "Control and optimal sizing of PV-Wind powered rural zone in Egypt", *Al-Azhar Engineering 10th International conference*, Cairo, Dec. 24-26, 2008.
- [7] S. Yerramalla, A. Davari, and A. Feliachi "Dynamic modeling and analysis of polymer electrolyte fuel cell", *IEEE Power Engineering Society Summer Meeting*, vol. 1, pp. 82-86, July 2002.
- [8] K. Sedghisigarchi, A. Feliachi, "Dynamic and transient analysis of power distribution systems with fuel Cells-part I: fuel-cell dynamic model", *IEEE Transactions on Energy Conversion*, vol. 9, no 2, pp. 423-428, 2004..

9. APPENDIX

Fuel Cell :	$\gamma_1 = 0.01$	$C_{d2} = 5000\mu F$
$V_{pm} = 240V$	$\gamma_2 = 0.01$	$C_{d3} = 5000\mu F$
$P_{pm} = 170KW$	$\gamma_3 = 0.1$	$R_d = 0.15\Omega$
$R_{r1} = 0.496\Omega$	$K_p = 5$	$L_d = 5e^{-3}H$
$R_{r2} = 1.508\Omega$	$K_i = 0.05$	PMDC Motor:
$R_m = 0.08074\Omega$	$K_d = 2$	$R_a = 1.5\Omega$
$R_s = 0.05\Omega$	Proposed Controller:	$L_a = 0.1H$
$C_1 = 1.55e^{-3}F$	$\gamma_1 = 20$	$J_0 = 14e^{-3}Kg.m^2$
$C_2 = 18.12e^{-3}F$	$\gamma_2 = 0.01$	$J_1 = 6.26e^{-5}Kg.m^2$
$L_s = 5e^{-3}H$	$\gamma_3 = 0.001$	$J_2 = 1.06e^{-6}Kg.m^2$
Battery :	$\gamma_S = 3.5$	$B_0 = 5.8e^{-3}N.m.s$
$V_{pm} = 240V$	$\gamma_I = 0.13$	$B_1 = 25e^{-6}N.m.s$
$R_{s1} = 0.05\Omega$	$\gamma_R = 0.83$	$B_2 = 0.42e^{-6}N.m.s$
$L_{s1} = 5e^{-3}H$	GPPF:	$K_e = 0.636$
PID Controller:	$C_{d1} = 5000\mu F$	$K_t = 0.636$